Scientific Research Publishing

Open Journal of Applied Sciences, 2024, 14, 2360-2373
https://www.scirp.org/journal/ojapps
ISSN Online: 2165-3925
ISSN Print: 2165-3917

Numerical Modelling of Coupled Heat and Mass Transfer in Porous Materials: Application to Cinder Block Bricks

Benjamin Kiema[1*], Ousmane Coulibaly[1], Xavier Chesneau[2], Belkacem Zeghmati[2]

[1]Laboratory of Environmental Physics and Chemistry (LPCE), Department of Physics, Joseph KI-ZERBO University, Ouagadougou, Burkina Faso
[2]Laboratory of Modelling Pluridisciplinary and simulation (LAMPS), University of Perpignan Via Domitia, Perpignan, France
Email: *benjaminkiema03@gmail.com

How to cite this paper: Kiema, B., Coulibaly, O., Chesneau, X. and Zeghmati, B. (2024) Numerical Modelling of Coupled Heat and Mass Transfer in Porous Materials: Application to Cinder Block Bricks. *Open Journal of Applied Sciences*, **14**, 2360-2373.
https://doi.org/10.4236/ojapps.2024.149156

Received: June 15, 2024
Accepted: September 6, 2024
Published: September 9, 2024

Abstract

In this work, we present numerical modelling of coupled heat and mass transfer within porous materials. Our study focuses on cinder block bricks generally used in building construction. The material is assumed to be placed in air. Moisture content and temperature have been chosen as the main transfer drivers and the equations governing these transfer drivers are based on the Luikov model. These equations are solved by an implicit finite difference scheme. A Fortran code associated with the Thomas algorithm was used to solve the equations. The results show that heat and mass transfer depend on the temperature of the air in contact with the material. As this air temperature rises, the temperature within the material increases, and more rapidly at the material surface. Also, thermal conductivity plays a very important role in the thermal conduction of building materials and influences heat and mass transfer in these materials. Materials with higher thermal conductivity diffuse more heat.

Keywords

Numerical Modelling, Coupled Transfer, Building Materials, Luikov Model, Finite Differences

1. Introduction

Heat and mass transfer in porous media are encountered in several natural or industrial phenomena, such as the infiltration of rainwater into soils and shrinkage. In the field of housing, effective management of heat and mass transfer through building materials is a fundamental element in guaranteeing the energy efficiency of buildings and ensuring their durability. Building materials, such as cinder block

bricks, have an important role in these transfers, having a direct impact on the comfort of occupants and the overall energy consumption of buildings [1].

Faced with these challenges, numerical modelling is emerging as an essential tool for accurately predicting heat and hygrothermal transfer phenomena in construction materials. Numerical several works were realised to analyse the influence of temperature and relative humidity of the ambient air on hygrothermal transfer in porous media. The main models of transfer in these porous media include the model by Crausse and al [2], which consists of calculating the spatial distribution of temperature and humidity in a building wall, the model by Philip and De Vries [3], which characterises heat and mass transfer in unsaturated porous media, the model by Luikov [4], which describes coupled transfer in hygroscopic porous media by highlighting the phenomenon of thermo-diffusion. This model establishes a gradient that causes moisture to move within the material. All these models have been applied to several types of conventional building materials such as wood [5], cement-mortar and sandstone [6], cork concrete [7]. This work is essential not only for characterising materials but also for accurately assessing building performance. Our study focuses on the development and application of numerical models to study coupled heat and mass transfer in a cinder block. In fact, cinder block is one of the most widely used materials used in construction, but its thermal and hygrothermal performance is highly dependent on various factors, such as its composition its porosity, and the environment in which it is stored and used [8]. Thus, the main objective of this research is to provide an in-depth understanding of the transfer mechanisms in cinder block, using numerical models based on the Luikov equations. This approach will make it possible to assess the impact of different parameters on the thermal and hygrothermal performance of the brick, paving the way to optimisation strategies aimed at improve the energy efficiency and durability of building structures.

2. Modelling Coupled Heat and Mass Transfer

The physical model is composed of a cinder block brick assimilated to a porous material of parallelepiped shape with dimensions ($40 \times 20 \times 15$ cm^3) placed in air (**Figure 1**). We assume that the height of the material is sufficiently greater than the other dimensions for heat and mass transfer to be two-dimensional. The vertical walls in contact with the air are subject to natural convection. The cartesian reference frame (xoy) associated with the physical model is such that the abscissa [ox) is counted positively from left to right; the axis [oy), perpendicular to [ox) is oriented in the opposite direction to gravity.

2.1. Mathematical Formulation and Resolution Procedure

2.1.1. Simplifying Model Assumptions

To solve the problem, we make the following assumptions:

- Heat and mass transfer are two-dimension
- The temperature and relative humidity of the air in which the material is placed are constant

- The material is assimilated to a homogeneous porous medium
- The material does not undergo any deformation over time
- Heat transfer by radiation is negligible

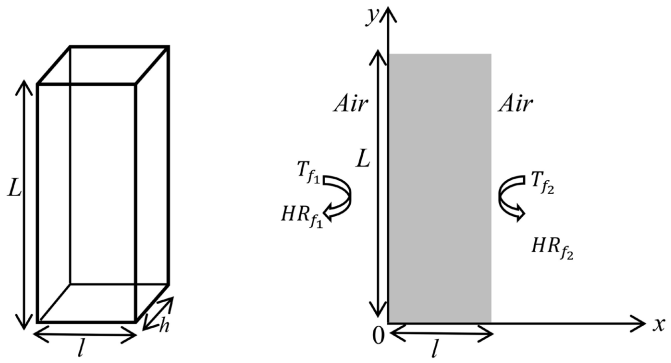

Figure 1. Physical representation.

2.1.2. Mathematical Equations

Taking into account the simplifying assumptions formulated above, the heat and mass transfer equations in the material, based on the Luikov model, can be written as follows in the cartesian referential (Oxy):

$$\begin{cases} \dfrac{\partial T_m}{\partial t} = D_T\left(\dfrac{\partial^2 T_m}{\partial x^2} + \dfrac{\partial^2 T_m}{\partial y^2}\right) + \dfrac{L_v \varepsilon}{C_p}\dfrac{\partial W_n}{\partial t} & (1) \\ \dfrac{\partial W_m}{\partial t} = D_m\left(\dfrac{\partial^2 W_m}{\partial x^2} + \dfrac{\partial^2 W_m}{\partial y^2}\right) + D_m\delta_s\left(\dfrac{\partial^2 T_m}{\partial x^2} + \dfrac{\partial^2 T_m}{\partial y^2}\right) & (2) \end{cases}$$

D_m : coefficient of mass diffusion of water in the material

D_T : coefficient of thermal diffusivity of heat in the material

δ_s : Thermo migration coefficient

L_v : latent heat of vaporization

ε : Rate of phase change

C_p : Specific heat

2.1.3. Initial and Boundary Conditions

- ***Initial conditions***

At $t \le t_0$; t (being the instant at which the interaction between the material and the surrounding environment begins).

$$T_m(x,y,t) = T_0\,(\text{Initial temperature of the material})$$

$$W_m(x,y,t) = W_0\,(\text{Initial moisture content of the material})$$

- ***Boundary conditions***

We assume that temperature and moisture content gradients are null on the horizontal faces. Heat and mass transfer take place only on the vertical faces of the material in contact with the surrounding environment.

For all $t < t_0$: we have:

$$y = 0;\quad 0 < x < l:$$

$$\left.\frac{\partial T_m}{\partial y}\right|_{y=0} = 0 \tag{3}$$

$$\left.\frac{\partial W_m}{\partial y}\right|_{y=0} = 0 \tag{4}$$

$y = L\ ;\ \ 0 < x < l$:

$$\left.\frac{\partial T_m}{\partial y}\right|_{y=L} = 0 \tag{5}$$

$$\left.\frac{\partial W_m}{\partial y}\right|_{y=L} = 0 \tag{6}$$

Air-material interface: Continuity of heat and mass flux densities

- $x = 0\ ;\ \ 0 \le y \le L \quad and \quad x = l\ ;\ \ 0 \le y \le L$

▪ ***Heat flux density***

$$-\lambda_m \left.\frac{\partial T_m}{\partial x}\right|_{x=0} = -\lambda_f \left.\frac{\partial T_f}{\partial x}\right|_{x=0} - (1-\varepsilon) L_v \rho_f D_f \left.\frac{\partial W_f}{\partial x}\right|_{x=0} \tag{7}$$

$$-\lambda_m \left.\frac{\partial T_m}{\partial x}\right|_{x=0} = ht_1 \left(T_f - T_m(0,y)\right) + (1-\varepsilon)\rho_f L_v h_m \left(w_{fs} - w_f\right) \tag{8}$$

λ_m : Thermal conductivity of the material

λ_f : Thermal conductivity of the fluid (air)

ρ_f : Density of the fluid (air)

w_{fs} : Water vapour concentration or dry water vapour content at the surface of the material

w_f : Water vapour concentration or dry-base water vapour content of air

h_t : convective heat transfer coefficient

The convective heat transfer coefficient ht is determined from the following corre lations [9]

$$Nu = 0.59 \cdot Ra^{1/4}$$

$$h_t = \frac{Nu \cdot \lambda_f}{L} = \frac{0.59 \cdot Ra^{1/4} \cdot \lambda_f}{L}$$

Nu: *Nusselt number*, *Ra*: *Rayleigh number*, λ_f : *Thermal conductivity of the fluid* (*air*)

▪ ***Mass flow density***

$$\rho_m D_m \left[\left.\frac{\partial W_m}{\partial x}\right|_x + \delta \left.\frac{\partial T_m}{\partial x}\right|_x\right] = \rho_f D_f \left.\frac{\partial W_f}{\partial x}\right|_x \tag{9}$$

D_f : *Water-vapour mass diffusion coefficient* ($m^2 \cdot s^{-1}$)

$$\rho_m D_m \left[\left.\frac{\partial W_m}{\partial x}\right|_x + \delta \left.\frac{\partial T_m}{\partial x}\right|_x\right] = \rho_f h_m \left(W_{fs} - W_f\right) \tag{10}$$

In Equations (8) and (10), W_{fs} is determined from the Henderson-type sorption

isotherm [10]: $H_r = 1 - \exp\left(-k \cdot T_m \cdot W_m^n\right)$ where H_r is the relative humidity, k and n are characteristic constants of the material determined experimentally, W_m is the dry-base moisture content.

2.1.4. Dimensionless Heat and Mass Transfer Equations

Equations (1, 2) and their associated initial and boundary conditions are dimensioned in order to generalize our results. These equations are dimensioned by the following dimensionless variables:

$$x^+ = \frac{x}{L}; y^+ = \frac{y}{L}; t^+ = \frac{D_T}{L^2}t; T_m^+ = \frac{T_m - T_0}{T_f - T_0}; W_m^+ = \frac{W_m}{W_0} \tag{11}$$

Introducing the above dimensionless variables into the heat and mass transfer equations leads to the following dimensionless equations:

$$\frac{\partial T_m^+}{\partial t^+} = \left(\frac{\partial^2 T_m^+}{\partial x^{+2}} + \frac{\partial^2 T_m^+}{\partial y^{+2}}\right) + \varepsilon \cdot Ko \frac{\partial W_m^+}{\partial t^+} \tag{12}$$

$$\frac{\partial W_m^+}{\partial t^+} = Lu\left(\frac{\partial^2 W_m^+}{\partial x^{+2}} + \frac{\partial^2 W_m^+}{\partial y^{+2}}\right) + Lu \cdot Pn\left(\frac{\partial^2 T_m^+}{\partial x^{+2}} + \frac{\partial^2 T_m^+}{\partial y^{+2}}\right) \tag{13}$$

$$Pn = \frac{\delta_s \Delta T}{W_o}: \text{Posnov number}$$

The Posnov number characterizes the relative influence of thermal diffusion in relation to the initial quantity of water present in the material. It can be used to assess the efficiency of heat transfer in a system where evaporation plays an important role.

$$Ko = \frac{W_o L_v}{\Delta T \cdot C_P}: \text{Kossovitch number}$$

This Kossovitch number is used in heat transfer and thermodynamics to describe the efficiency of heat transfer in terms of phase change.

$$Lu = \frac{D_m}{D_T}: \text{Luikov number}$$

Luikov number is used to describe the relationship between heat propagation and mass propagation in a material.

Boundary conditions (3, 4, 5, 6, 8, 10) are written in dimensionless form:

$$x^+ = 0; 0 \le y^+ \le L^+ \text{ and } x^+ = \frac{l}{L}; 0 \le y^+ \le L^+$$

- **Heat and mass flux density**

$$\left.\frac{\partial T_m^+}{\partial x^+}\right|_{x^+, y^+} = Bit\left(T_m^+ - 1\right) - Ad\left(W_{fs} - W_f\right) \tag{14}$$

$$\left.\frac{\partial W_m^+}{\partial x^+}\right|_{x^+, y^+} + Pn\left.\frac{\partial T_m^+}{\partial x^+}\right|_{0, y^+} = \frac{\rho_f}{W_0 \rho_m} Bim\left(W_{fs} - W_f\right) \tag{15}$$

$$Ad = \left(1 - \varepsilon\right)\frac{L \cdot h_m \cdot \rho_f \cdot L_v}{\lambda_m\left(T_f - T_0\right)}$$

$Bit = \frac{Lh_t}{\lambda_m}$: Biot number of heat transfer

$Bim = \frac{Lh_m}{D_m}$: Biot number of mass transfer

The convective mass transfer coefficient h_m is determined from the following correlations [11]

$$h_m = \frac{Sh \cdot D_f}{L}$$

$$Sh = 0.59 \cdot \left(Gr_m \cdot Sc\right)^{1/4}$$

Sh: Sherwood number

D_f: mass diffusion coefficient water vapour

Gr_m: Grashof number of mass transfer

Sc: Schmidt number

$$y^+ = 0; 0 \le x^+ \le \frac{l}{L} \text{ and } y^+ = L; 0 \le x^+ \le \frac{l}{L}$$

- **Heat and mass flux density**

$$\left.\frac{\partial T_m^+}{\partial y^+}\right|_{y^+} = 0 \quad (16)$$

$$\left.\frac{\partial W_m^+}{\partial y^+}\right|_{y^+} = 0 \quad (17)$$

3. Numerical Resolution

The heat and mass transfer equations and their associated initial and boundary conditions were discretised using the implicit finite difference method and solved using a Fortran code and the Thomas algorithm. The convergence criterion we have adopted is equal to 1×10^{-3} and a sub-relaxation coefficient of 7×10^{-1}.

4. Thermophysical Properties of the Material Studied

Most of the thermophysical properties (Table 1) of the material under study were determined using the KD2-Pro device in our previous work [8].

Table 1. Thermophysical properties of the material.

Material	λ (W/m·K)	ρ (kg/m³)	C_P (J/kg·K)	α (m²/s)
Cinder block	1.32	2150	1818	3.86×10^{-7}

5. Results and Discussion

5.1. Validation of Results

To ensure that our program is valid, we compared our results with some results from the literature. The temperature and water content distributions determined numerically by the Luikov model, for a heat and mass transfer problem, are

compared with those obtained by M. SAIDI *et al.* [12] in a biosourced building material of the BTC type (compressed earth bricks). Figure 2 and Figure 3 show the validation results.

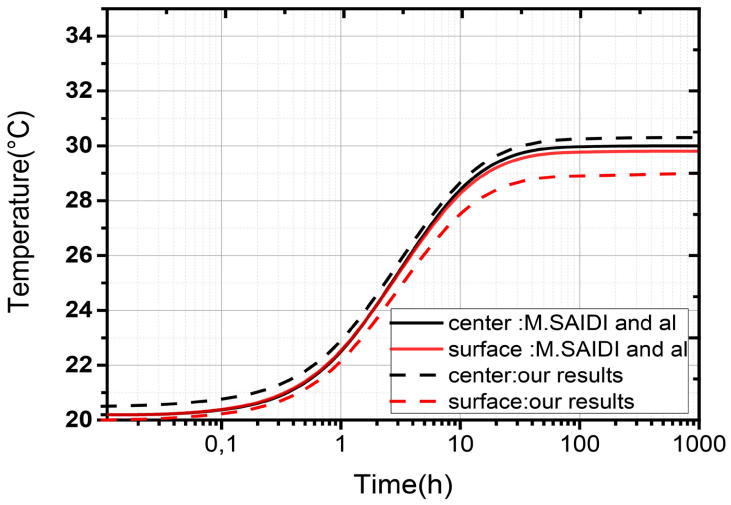

Figure 2. Temperature at the center and surface of cinder block specimen.

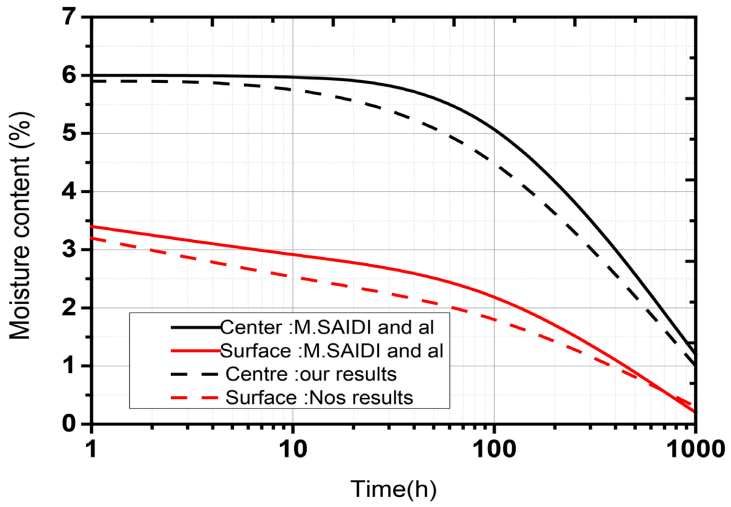

Figure 3. Moisture content at the center and surface of cinder block specimen.

The agreement between our results and those of M. SAIDI and al assures us of the validity of our code for the problems of estimating the temperature and water content distributions in our porous material.

5.2. Mesh Sensitivity

A sensitivity study was carried out for three different mesh sizes 67× 101, 76 × 151, 51 × 101. The results of this study are obtained by comparing the values of temperature and moisture content at the outer face ($x = 0$) and inner face ($x = 1$) of the material, where the temperature and moisture gradients are greatest. The

results obtained show that the maximum error between the temperature and water content values is of the order of 10^{-3} between these three meshes. Consequently, we adopted the 51 × 101 mesh.

5.3. Values of the Initial Conditions for the Simulation

At the initial time, the temperature T_0 and the water content of the material W_0 are taken to be equal to T_0 = 22˚C and W_0 = 0.12 kg water/kg respectively. The two vertical faces of the material are maintained at temperatures T_{f1} = 40˚C and T_{f2} = 30˚C. The relative humidity of the air in contact with these surfaces is 20%. The thermo-physical properties and Henderson desorption isotherm coefficients of the material used in the calculations are given in Table 1 and Table 2.

Table 2. Desorption isotherm coefficients according to the Henderson model.

Desorption isotherm coefficients	k	n
T = 35˚C	1.5	1.047
T = 40˚C	0.718	0.813
T = 50˚C	5.199	1.533

5.4. Temperature and Moisture Content Profiles

Figure 4 and Figure 5 shows the temporal evolution of the temperature and moisture content at the center and surface of the material. It can be seen that the temperatures at the center and surface of the material increase over time until they reach a constant value close to the temperature of the fluid (air). This change in material temperature is due to natural convection between the fluids and the material.

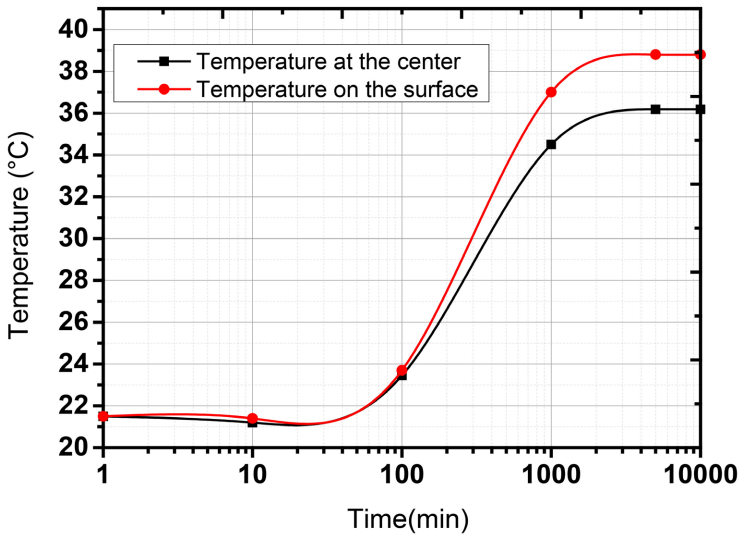

Figure 4. Temperature at the center and surface of the cinder block specimen.

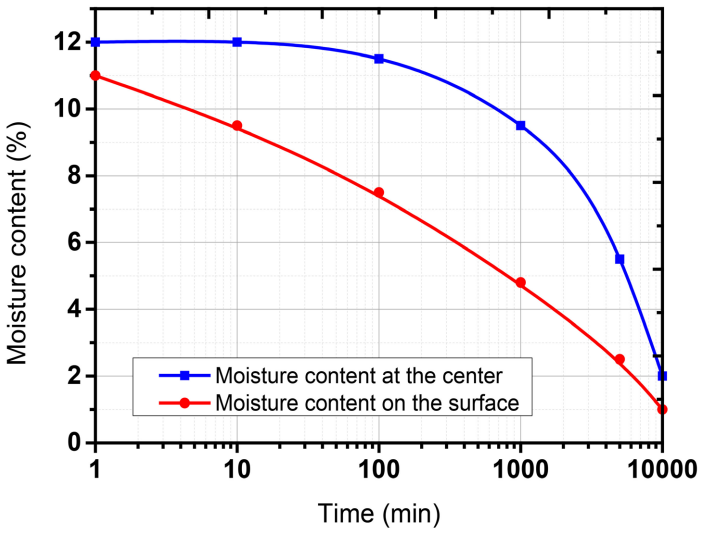

Figure 5. Moisture content at the center and surface of the cinder block.

Figure 4 shows the evolution of the temperature at the center and at the surface of the material. Over a period of 60 minutes (1 hour), the temperature at the center and at the surface of the material are almost identical and equal to its initial temperature. This is because the quantity of heat supplied by convection in sensible form by the air, combined with the thermal inertia of the material, is not sufficient to cause evaporation of the free water at the surface of the material, which could have an impact on the evolution of the temperature. Over time, the temperatures at the center and surface of the material change due to the effect of the latent heat in the air, which causes the water to evaporate very quickly. Almost 5 days (7000 min) later, the temperatures at the center and surface of the material each reach an almost asymptotic maximum value, marking the complete evaporation of the free water. During this drying period, the porous material is in thermal equilibrium with the drying air. In this state, the material has fully hardened and is ready for use in construction.

Figure 5 shows the evolution of moisture in the material over time, represented at the center and at the surface of the material. It can be seen that at the start of the process, the moisture content in the center of the material is slightly higher (0.12 kg/kg) than at the surface (0.11 kg/kg). This can be explained by the fact that water generally accumulates more in the center during the manufacture or storage of the material. Before 60 min of drying, the moisture content in the center of the material remains constant because the air temperature does not allow considerable evaporation of free water, but it nevertheless has an impact on the surface of the material. After 100 minutes, the addition of heat by convection from the air causes the water to migrate from the center to the surface of the material, where it evaporates, causing the moisture content in the center to fall. It can be seen that throughout the drying process, the decrease in moisture at the surface of the material over time is greater than that in the middle, because the evaporation of water at the surface is mainly governed by the gradient in water vapour concentration

between that at the surface and that of the air in which the material is placed.

5.5. Influence of Air Temperature on Temperature and Moisture Content at the Center of the Cinder Block

Figure 6 and Figure 7 were obtained by considering different values of air temperature (face1). We analyse the influence of the air temperature T_{f1} (35˚C, 40˚C and 50˚C) on the spatio-temporal distributions of temperature and moisture content in the brick.

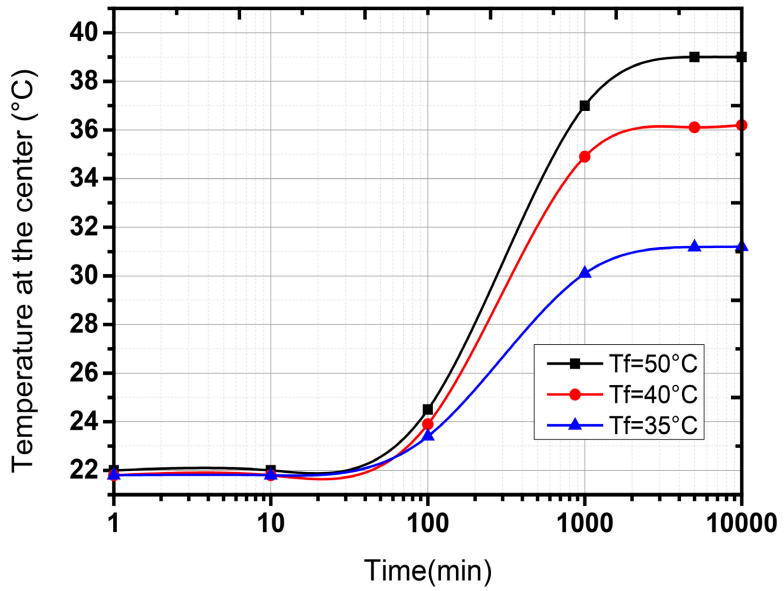

Figure 6. Influence of air temperature on the temperature at the center of the cinder block.

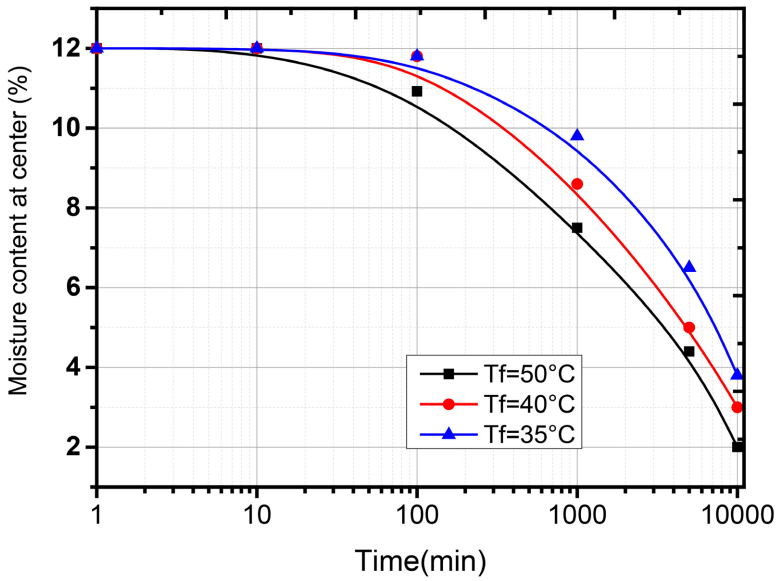

Figure 7. Influence of air temperature on moisture content at the center of the cinder block.

Figure 6 shows the temperature profiles at the center of the cinder block sample. It can be seen that after each increase in outside air temperature, the temperature at the center of the material tends to rise rapidly. This rise is due to heat transfer by convection at the surface and by conduction within the material. This confirms the effect of air temperature on heat transfer within porous materials. This phenomenon was also observed in the work of [13] on wood, in which the material was subjected to a very high temperature, which considerably affects the temperature within the material and precipitates the drying time. It is therefore important to select a drying temperature that maintains the quality of the material, as too high a temperature can degrade the material, affecting its final quality. This is particularly important for heat-sensitive materials [14].

The curves in Figure 7 show the changes in water content at three different air temperatures (35˚C, 40˚C and 50˚C) in the center of the material. At the start of drying (between 1 and 10 minutes), the water content is practically the same for all three drying temperatures. This indicates that there is almost no migration of water from the center to the surface of the material [15]. Analysis of the figure shows that for three different drying temperatures, the water content in the center of the material decreases over time. However, this decrease in water content is more rapid for very high temperatures. According [16], the drying rate of a product is proportional to the temperature difference between the material and the surrounding air. After 100 min, the water content for an air temperature of 50˚C becomes lower, illustrating the effect of the drying temperature in accelerating water evaporation. This could be due to the increase in thermal energy available to break the bonds between the water and the material.

5.6. Effect of Thermal Conductivity on Temperature and Moisture Content at the Center of the Material

Thermal conductivity plays a very important role in the thermal conduction of building materials and influences heat and mass transfer in these materials. Figure 8 and Figure 9 show the influence of this parameter on hygrothermal transfer.

Figure 8 shows the temperature at the center of the material as a function of time for different values of thermal conductivity. At the beginning (0 - 1000 min), all three curves show a rapid increase in temperature. This phase indicates that the material is heating up rapidly due to the evaporation of free water from the surface of the material. After 3000 minutes, the temperature at the center of the material for all three values of thermal conductivity stabilize, indicating that the material has reached thermal equilibrium. Materials with high thermal conductivity heat up more quickly and reach a higher temperature, making them suitable for applications requiring efficient heat transfer. This same phenomenon was observed in the work of [17] for different types of concrete with different thermal conductivity values. These materials are ideal for applications where rapid heat dissipation is required [18]. Conversely, low thermal conductivity materials are better suited to insulation applications.

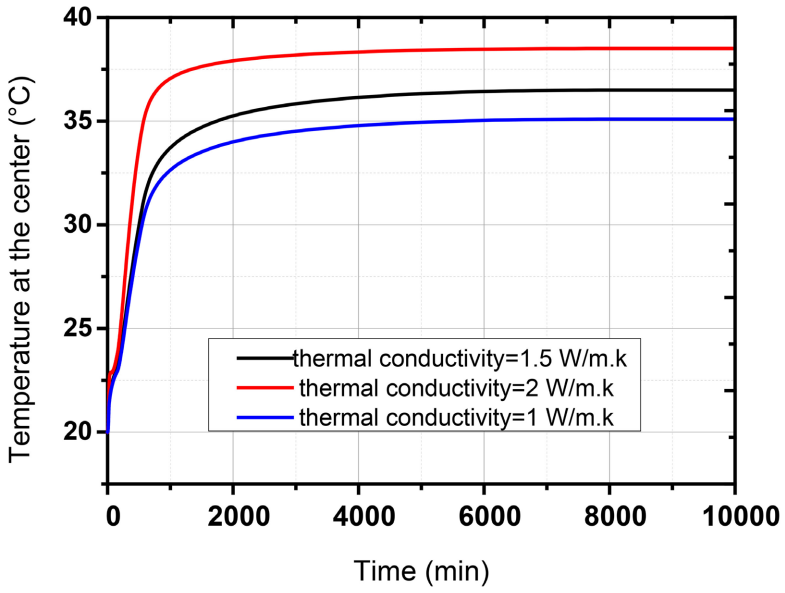

Figure 8. Effect of thermal conductivity on the temperature at the center of the cinder block.

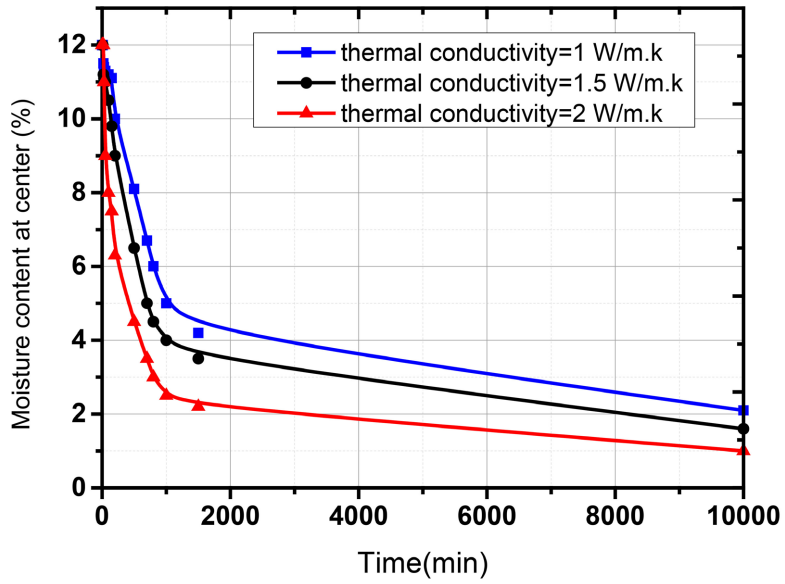

Figure 9. Effect of thermal conductivity on moisture content at the center of the cinder block.

Figure 9 shows that for all three thermal conductivities, the moisture content decreases over time, indicating a drying process where the material loses moisture content over time. It can be seen that the moisture content decreases faster for materials with a higher thermal conductivity and reaches a lower equilibrium moisture content compared to those with a lower thermal conductivity. A similar observation was made in the work of [19]. The authors mention that the improvement in thermal conductivity facilitates faster evaporation of water thanks to more efficient heat distribution. This could be due to the migration of liquid water from

the center to the surface of the material under the effect of the fluid temperature [20]. In addition, materials with a higher thermal conductivity show a faster initial drying rate and reach equilibrium more quickly [21].

6. Conclusion

We have carried out a numerical analysis of the thermo-hydric behaviour of cementitious construction materials. The heat and mass transfer equations are based on the Luikov model. These equations were solved using an implicit finite difference method and the Thomas algorithm. The results show that heat and mass transfer are strongly influenced by air temperature. The greater the temperature of the air in which the material is placed, the greater the decrease over time in the moisture content of the material. It should also be noted that air temperature and thermal conductivity play a very important role in determining the drying efficiency of materials. Higher temperatures reduce moisture content more quickly, but this must be balanced against considerations of material quality and energy consumption. Our study has been limited to the application of Luikov's model to cinder blocks, but we intend to extend it to other building materials, and we intend to impose a heat flow on the surface of the material in order to analyze its influence on the hygrothermal parameters of the material.

Acknowledgements

This research work is the fruit of a collaboration between the Joseph KI-ZERBO University (Burkina Faso) and the University of Perpignan Via Domitia (France). I would like to thank the French Embassy in Burkina Faso for granting me a scholarship that enabled me to travel to France for study.

Conflicts of Interest

The authors declare no conflicts of interest regarding the publication of this paper.

References

[1] Sawadogo, D. and Coulibaly, O. (2021) Comparative Study of the Thermal Comfort of Four Materials Type Used in the Construction of a Building. *Journal of Energy and Power Engineering*, **15**, 231-242. https://doi.org/10.17265/1934-8975/2021.07.001

[2] Crausse, P., Bacon, G. and Bories, S. (1981) Etude fondamentale des transferts couples chaleur-masse en milieu poreux. *International Journal of Heat and Mass Transfer*, **24**, 991-1004. https://doi.org/10.1016/0017-9310(81)90130-7

[3] Philip, J.R. and Devries, D.A. (1957) Moisture Movement in Porous Materials under Temperature Gradients. *Transactions American Geophysical Union*, **38**, 222-232.

[4] Luikov, A.V. (1975) Systems of Differential Equations of Heat and Mass Transfer in Capillary-Porous Bodies (Review). *International Journal of Heat and Mass Transfer*, **18**, 1-14. https://doi.org/10.1016/0017-9310(75)90002-2

[5] Abahri, K., Belarbi, R. and Trabelsi, A. (2011) Contribution to Analytical and Numerical Study of Combined Heat and Moisture Transfers in Porous Building

Materials. *Building and Environment*, **46**, 1354-1360. https://doi.org/10.1016/j.buildenv.2010.12.020

[6] Qin, M., Aït-Mokhtar, A. and Belarbi, R. (2010) Two-Dimensional Hygrothermal Transfer in Porous Building Materials. *Applied Thermal Engineering*, **30**, 2555-2562. https://doi.org/10.1016/j.applthermaleng.2010.07.006

[7] Sotehi, N. and Chaker, A. (2014) Numerical Analysis of Simultaneous Heat and Mass Transfer in Cork Lightweight Concretes Used in Building Envelopes. *Physics Procedia*, **55**, 429-436. https://doi.org/10.1016/j.phpro.2014.07.062

[8] Kiema, B., Coulibaly, O. and Ouedraogo, E. (2024) Study of the Influence of Storage Media on the Thermo-Mechanical Behavior of Concrete and Cement Blocks. *Physical Science International Journal*, **28**, 45-55. https://doi.org/10.9734/psij/2024/v28i1820

[9] Padet, J. (2015) Convection thermique et massique. Nombre de Nusselt: Partie 1, technique de l'ingénieur, BE8206, p. 24.

[10] Henderson, S.M. (1952) A Basic Concept of Equilibrium Moisture. *Agricultural Engineering*, **33**, 29-32.

[11] Lienhard IV, J.H. and Lienhard V, J.H. (2005) A Heat Transfer Textbook. 3rd Edition, Phlogiston Press.

[12] Saidi, M., Cherif, A.S., Sediki, E. and Zeghmati, B. (2017) Analyse Numérique du Comportement Thermo-Hydrique de Briques de Terre Stabilisée au Ciment. *Chez* 5*ème Conférence Internationale des Energies Renouvelables* (*CIER*-2017), Vol. 31, 1-6.

[13] Younsi, R., Kocaefe, D. and Kocaefe, Y. (2006) Three-Dimensional Simulation of Heat and Moisture Transfer in Wood. *Applied Thermal Engineering*, **26**, 1274-1285. https://doi.org/10.1016/j.applthermaleng.2005.10.029

[14] Vega-Mercado, H., Góngora-Nieto, M.M. and Barbosa-Cánovas, G.V. (2001) Advances in Drying and Dehydration of Foods. *Food Engineering*: *Integrated Approaches*, **2**, 255-284.

[15] Qin, M.R. Belarbi, R., Aït-Mokhtar, A. and Seigneurin, A. (2006) An Analytical Method to Calculate the Coupled Heat and Moisture Transfer in Building Materials. *International-Communications in Heat and Mass Transfer*, **33**, 39-48. https://doi.org/10.1016/j.icheatmasstransfer.2005.08.001

[16] Mujumdar, A.S. (2007) Handbook of Industrial Drying. 3rd Edition, CRC Press.

[17] Oudrane, A., Aour, B., Zeghmati, B. and Chesneau, X. (2019) Étude numérique de diffusion thermique dans un système de stokage d'énergie destiné pour le chaufage par le sol: Cas de la dalle plancher. *African Review of Science*, *Technology and Development*, **4**, 46-56.

[18] Incropera, F.P., DeWitt, D.P., Bergman, T.L. and Lavine, A.S. (2007) Fundamentals of Heat and Mass Transfer. John Wiley & Sons.

[19] Wang, Y. and Zhao, C. (2023) Impact of Thermal Conductivity on Drying Kinetics of Porous Materials. *Chemical Engineering Science*, **248**, 240-250.

[20] Li, H. and Chen, L. (2021) Equilibrium Moisture Content in Drying Processes: Effects of Thermal Conductivity. *International Journal of Heat and Mass Transfer*, **179**, 180-193.

[21] Zhang, X. and Liu, J. (2022) Thermal Conductivity and Its Impact on Drying Dynamics of Construction Materials. *Drying Technology*, **40**, 813-822.